Tungsten in silicon carbide: Band-gap states and their polytype dependence

N. Achtziger,[1,*] G. Pasold,[1,†] R. Sielemann,[2] C. Hülsen,[1] J. Grillenberger,[1] and W. Witthuhn[1]
[1]*Institut für Festkörperphysik, Friedrich-Schiller-Universität Jena, Max-Wien-Platz 1, D-07743 Jena, Germany*
[2]*Hahn-Meitner-Institut Berlin, Glienicker Straße 100, D-14109 Berlin, Germany*
(Received 30 May 2000)

Band-gap states of tungsten in silicon carbide (polytypes $4H$, $6H$, and $15R$) are investigated by deep-level transient spectroscopy (DLTS) and admittance spectroscopy on *n*-type SiC. Doping with W is done by ion implantation and annealing. To establish a definite chemical identification of band-gap states, the radioactive isotope ^{178}W is used as a tracer: band-gap states involving a ^{178}W isotope are uniquely identified by their decreasing concentration during the nuclear transmutation of ^{178}W to Hf. In addition, conventional doping studies with stable W isotopes are performed. Within the part of the band gap accessible by DLTS on *n*-type SiC, there is one tungsten-related deep level with a large capture cross section (10^{-12} cm^2) for electrons. In the polytypes $4H$, $6H$, and $15R$, its energy is 1.43, 1.16, and 1.14 eV below the conduction-band edge (E_C), respectively. The polytype dependence of this level position directly reflects the conduction-band offset. In the $4H$ polytype, an additional level close to the conduction band ($E_C-0.17$ eV) exists that is absent in the other polytypes because of their smaller band gap. Due to the acceptorlike deep band-gap state, tungsten is a good candidate for a compensating center to produce semi-insulating SiC.

I. INTRODUCTION

Silicon carbide (SiC) is one of the wide-gap semiconductors that attract great interest in current semiconductor research and development.[1,2] Because of excellent material properties,[3] it is expected to replace Si or GaAs in high-power[4] or high-frequency[5] electronics and to enable new applications in rough environments and at high temperature.[6] Silicon carbide exists in a variety of crystallographically different polytypes. The great majority of research and development focuses on two hexagonal polytypes, $4H$ and $6H$. The third polytype of our study, $15R$, is less well investigated. Very recently, rather good channel mobilities in metal-oxide semiconductor field-effect (MOS) transistors were obtained with this polytype[7] that will attract further interest.

Electronic properties of semiconductors are generally extremely sensitive to minor traces of impurities that create energy levels in the band gap. Consequently, there is a general interest to reveal the correlation between a certain element or defect and its band-gap states. This knowledge is the necessary basis to either identify impurities in a given material by detecting their band-gap states or to adjust material properties by intentional doping with a certain element. For the element tungsten in SiC, both aspects are important. Due to its extreme thermal stability, tungsten is a potential material for crystal-growth equipment and may thus become a possible contamination in SiC. This situation is similar to the neighboring element tantalum, which is already being used for the growth of bulk crystals[8,9] as well as epitaxial layers.[10] Band-gap states of tantalum were recently identified in an analogous study.[11] In addition, there is a general and continuous interest in deep band-gap states that may serve as compensating centers in order to produce semi-insulating SiC substrates for high-frequency devices.[12] The deep level of tungsten detected in the present study turns out to be a good candidate for this purpose. To our knowledge, no information on the properties of W in SiC is available in the literature up to now.

In the present study, doping with tungsten is done by ion implantation and annealing. Subsequently, band-gap states are analyzed by deep-level transient spectroscopy[13,14] (DLTS) and by thermal admittance spectroscopy[15,16] (TAS). In order to avoid any confusion between tungsten-related levels and intrinsic or implantation-induced defects, a radioactive isotope of tungsten (^{178}W) is used as a tracer. By performing several subsequent DLTS measurements during its nuclear decay (half-life 22 d), tungsten-related band-gap states are uniquely characterized by a decreasing concentration, whereas all other band-gap states remain unaffected. This ''radiotracer'' concept in combination with DLTS has already been used to identify impurity-related levels in silicon[17] and silicon carbide (e.g., Ti, V, Cr).[18,19] Reviews of experiments and methodical aspects are available.[20,21]

II. EXPERIMENTAL PROCEDURE

Doping experiments with stable tungsten isotopes were done on three polytypes ($4H$, $6H$, and $15R$) and additional radiotracer experiments on $4H$- and $6H$-SiC. We used commercial (Cree, Inc.) *n*-type epitaxial layers on heavily doped (5×10^{18} cm^{-3}) *n*-type substrates (*n*-type dopant nitrogen). For the polytypes $4H$, $6H$, and $15R$, the net shallow doping level of the epitaxial layers was in the range of (5–9), (3–6), and $(1-2)\times10^{15}$ cm^{-3}, respectively. The $15R$ material was taken from an unintentional inclusion in a nominal $6H$ crystal. Polytype determination was done by Raman spectroscopy.

A. Implantation of stable W isotopes

Ion implantation of stable W isotopes was performed at the tandetron accelerator JULIA in Jena at room temperature with multiple energies between 1.0 and 6.2 MeV to obtain an approximately homogenous W concentration of 2×10^{14} cm^{-3} in a depth between 0.2 and 1.2 μm (for details, see Ref. 11). This impurity concentration is about one order of magnitude less than the shallow doping level, which is an

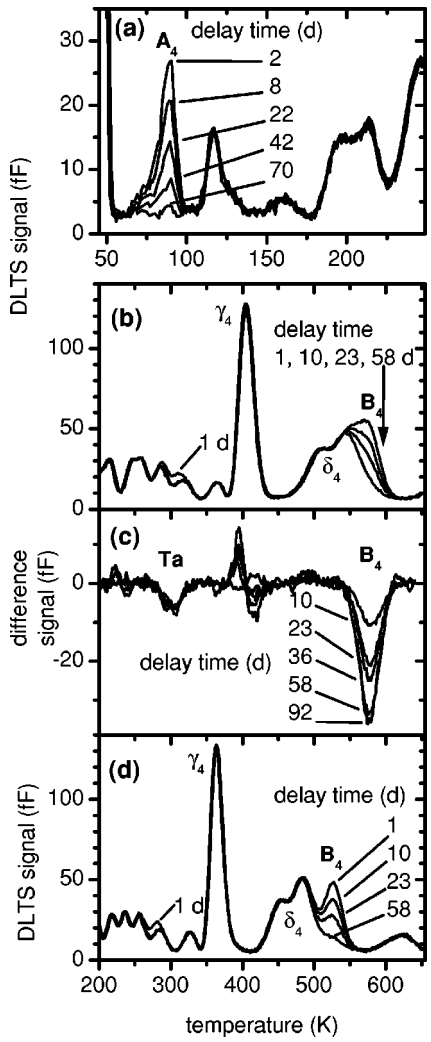

FIG. 1. DLTS spectra of *n*-type 4*H*-SiC taken sequently during the transmutation of ^{178}W to Hf ($U_R = 15$ V, $U_P = 1$ V, i.e., relative pulse height = 14 V). (a, b) Low- and high-temperature parts of the spectra (standard reference time constant $\tau_{ref} = 12.4$ ms). (c) Difference of spectra from (b). The initial spectrum is subtracted from all sequentially measured spectra. (d) Same as (b), but measured with a longer DLTS time window ($\tau_{ref} = 237$ ms) in order to better separate the time-dependent peak B_4 from the background.

optimum condition for DLTS. In the polytype 4*H*, additional samples were implanted with a fluence increased by a factor of 20, optimized for TAS measurements.

B. Properties and implantation of the radiotracer isotope ^{178}W

The isotope ^{178}W used as a radioactive tracer transmutes to stable ^{178}Hf in two steps. The first decay to ^{178}Ta with a half-life of 22 d determines the time scale of the experiment. The daughter nucleus ^{178}Ta is unstable and quickly decays to stable ^{178}Hf with a half-life of at most 2.5 h. Due to the comparatively fast second decay, there is no accumulation of nuclei in the intermediate ^{178}Ta state. Hence, for the present purpose of a radiotracer experiment, the transmutation may simply be regarded as a W→Hf transmutation with a half-life of 22 d.

The desired isotope ^{178}W was recoil implanted[22] at the Cyclotron of the Hahn-Meitner-Institute in Berlin: a primary beam of 95-MeV $^{18}O^{4+}$ ions induces nuclear reactions in a holmium target foil (thickness 1.5 μm). The reactions products are kicked out of the foil with recoil energies on the order of some MeV. The samples to be implanted are mounted off-axis to the primary beam behind the target foil[22] and are thus implanted with the recoiling reaction products and, inevitably, also with stable Ho atoms kicked out of the foil without nuclear transformation.

The compound nucleus formed by fusion of ^{18}O and ^{165}Ho is ^{183}Re. It instantaneously emits about 5 nucleons, preferentially neutrons, to end up as a neutron-deficient, β^+-unstable reaction product that will decay along its β-decay chain.[23] Both the reaction paths ^{165}Ho(^{18}O,5*n*)^{178}Re→^{178}W as well as ^{165}Ho(^{18}O,*p*4*n*)^{178}W produce the desired isotope ^{178}W. Competing reaction channels will result in isotopes with adjacent mass numbers $A = 177$ and eventually $A = 179$. For the present experiment, however, only nuclei with half-lives on the order of 10 d are relevant. There is no such nucleus in the $A = 179$ decay chain and one nucleus, ^{177}Ta, in the $A = 177$ chain. This isotope decays to stable Hf with a half-life of 2.4 d and was recently used in a similar radiotracer experiment to identify band-gap states of Ta in 4*H*-SiC.[11] Experimentally, the mixture of isotopes implanted was investigated by γ-ray spectroscopy on each implanted sample. Characteristic γ rays[24] of the desired isotope ^{178}W, of its intermediate decay state ^{178}Ta, and of ^{177}Ta were detected. From the γ activity, an initial implantation fluence of 1.5×10^{10} cm^{-2} for ^{178}W and 0.5×10^{10} cm^{-2} for ^{177}Ta is derived. Due to the nuclear decay, the amount of ^{177}Ta is reduced by a factor of 2 at the time of the first DLTS measurements, i.e., the initial concentration ratio of the desired ^{178}W relative to the coimplanted ^{177}Ta is about 6.

C. Annealing and diode preparation

After implantation, the samples were annealed in sealed quartz ampoules filled with oxygen at 1600 K for 4 h (process motivated in Ref. 18). After removing the resulting sacrificial oxide layer in hydrofluoric acid, Schottky contacts (0.5 mm diameter) were produced by evaporation of nickel onto the implanted epitaxial layer. A titanium layer evaporated onto the substrate served as Ohmic contact. Leakage currents at 10 V reverse bias were typically below 1 nA at 300 K and on the order of 1 μA at the highest measuring temperature of 650 K. According to γ-ray spectroscopy done on completely prepared samples, there is no loss of ^{178}W during annealing or diode preparation.

D. Characterization techniques

Detailed explanations of DLTS[14,25,26] and TAS[15,16] may be found in the literature. The DLTS spectra were recorded by a commercial digital DLTS system.[27] During one temperature scan with a rate of typically 0.06 K/s, capacitance transients were recorded within several predefined time windows (5 ms, 100 ms, and 2 s). Several settings of reverse bias U_R (up to 15 V) and pulse bias voltage U_p were chosen, depending on the net shallow doping level of the samples. The main goal was to analyze a depth region between about

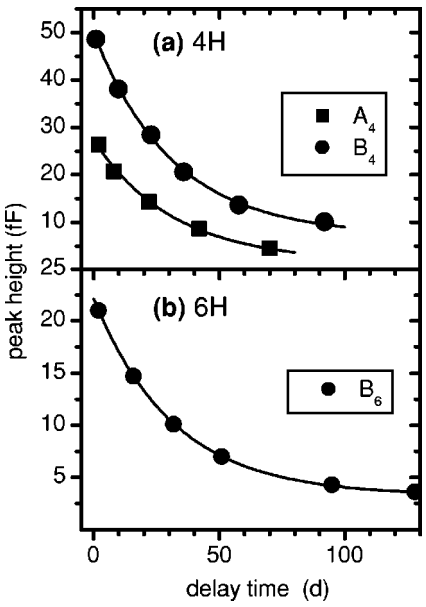

FIG. 2. Time dependence of the DLTS peak height in (a) 4*H*-SiC and (b) 6*H*-SiC during the W→Hf transmutation. The lines are exponential decay functions with a fixed half-life of the nuclear decay (22 d). The peak height data are taken from the spectra shown in Figs. 1(a), 1(d), and 4(b).

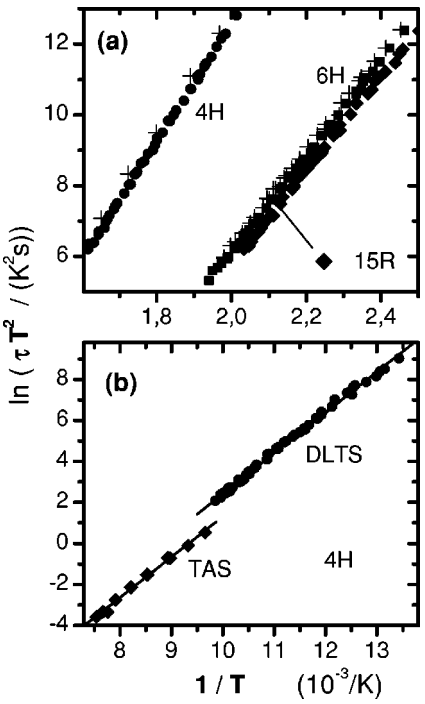

FIG. 3. Arrhenius plot of the (T^2-corrected) electron-emission time constant τ of tungsten related levels in *n*-type SiC. (a) Level *B* in three different polytypes. The crosses represent data obtained from radiotracer experiments (difference spectra in the case of polytype 4*H*). The other symbols are from samples doped with stable W isotopes. (b) Level A_4 in the polytype 4*H*. Additionally, the relaxation time constant obtained from TAS is included ($\tau = 1/\omega$). The slope of the straight lines corresponds to a thermal activation energy of 0.17 eV. The vertical offset between the two lines corresponds to a multiplication factor of $\frac{1}{3}$ (TAS relative to DLTS data).

0.4 and 1.2 μm. The trap parameters energy E_T and capture cross section σ (assumed to be independent of temperature) were derived as usual[14] from an Arrhenius plot of $\ln(T^2\tau)$, covering 3 orders of magnitude of the time constant τ (1 ms–1 s); T denotes the peak temperature. The errors given for the trap energy include only those errors influencing the slope of the Arrhenius plot, but not systematic uncertainties[14] of DLTS.

Unless otherwise mentioned, all DLTS spectra shown were taken with a pulse length of 1 ms and a predefined time window of 100 ms; the peak positions refer to a time constant τ_{ref} of 12.4 ms; the peak height equals the amplitude of the capacitance transient. TAS spectra were taken with a Keithley 3330 *LCZ* meter with ac frequencies *f* between 0.3 and 100 kHz at a reverse bias of 2 V.

III. RADIOTRACER-DLTS EXPERIMENTS

DLTS spectra were taken several times during the transmutation of ^{178}W to Hf as shown in Fig. 1 for one 4*H* sample (out of six sequences measured on six contacts on three different samples). In the polytype 4*H*, DLTS spectra at low temperatures were taken separately as shown in Fig. 1(a). One peak at 88 K, labeled A_4, clearly vanishes during the transmutation, whereas other peaks remain constant. The height of this peak exponentially decreases with delay time as shown in Fig. 2(a). This decrease is well described by a half-life of 21 ± 3 d. The close match with the nuclear half-life of ^{178}W immediately demonstrates that the corresponding band-gap state is due to a defect that involves exactly one W atom. The standard DLTS analysis of this peak (Fig. 3) reveals a trap energy of 0.17(1) eV and a capture cross section of $\sigma = 3 \times 10^{-14}\,\mathrm{cm}^2$.

In the high-temperature DLTS spectra shown in Fig. 1(b), there is also a decreasing signal, labeled B_4, that appears superimposed on a stable background. This background signal δ_4 exists in the radiotracer samples only; it consists of at least two peaks that cannot be separated reliably and will not be discussed here. By choosing a longer DLTS time window of 2 s [Fig. 1(d), $\tau_{\mathrm{ref}} = 237$ ms], the decreasing signal B_4 appears as a well-resolved peak. To extract peak positions and decay information also from the spectra taken at shorter time windows, it is well justified to form differences between subsequently measured spectra (DLTS spectra depend linearly on concentrations in the present case of low trap concentrations). The resulting difference spectra [Fig. 1(c)] clearly exhibit one negative peak at 570 K reflecting the decreasing DLTS signal at the same temperature. Several difference spectra were calculated for a set of different time windows and correlation functions (not shown) to cover the full range of time constants for the Arrhenius plot of the DLTS evaluation [crosses in Fig. 3(a)]. The result is a trap energy of 1.43 eV for 4*H*-SiC and a large capture cross section of about $10^{-12}\,\mathrm{cm}^2$ (Table I). The peak height versus delay time dependence of peak B_4 again closely follows the nuclear decay law as shown in Fig. 2(a) and thus proves the involvement of one W atom in this level.

In addition to the peak at 570 K, the difference spectra exhibit some scatter around 400 K with no obvious correlation to delay time, which results from taking differences for the large peak labeled γ_4. At 300 K, however, there is a significant and reproducible decrease in the DLTS spectra,

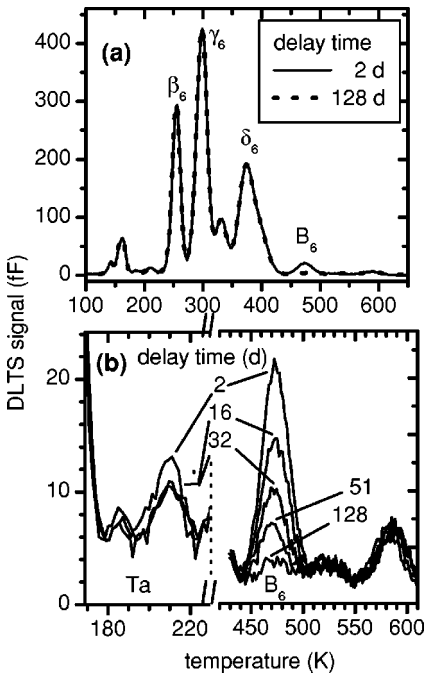

FIG. 4. (a) DLTS spectra of *n*-type 6*H*-SiC taken sequently during the transmutation of ^{178}W to Hf ($U_R = 10$ V, $U_P = 0.5$ V). Interesting details are enlarged in (b).

which appears as one distinct peak in the difference spectra. The time scale of this effect is short; it is completely finished within 10 d (all subsequent spectra are identical). With peak positions determined from the difference spectra as described above, this peak corresponds to an apparent energy of 0.62 eV and a capture cross section of 10^{-14} cm^2. These values exactly correspond to the result obtained recently for the band-gap state of tantalum in a similar experiment[11] using ^{177}Ta intentionally. Since the present samples also contain ^{177}Ta, the occurrence of this peak is expected. The relative height of the Ta and W related peaks in the difference spectra of about 1:5 (averaged over several samples) reasonably corresponds to the concentration ratio of ^{177}Ta to ^{178}W of 1:6 determined from γ-ray spectroscopy (Sec. II B). Corrected for its electric field dependence, the energy of the Ta level[11] is $E_C - 0.68(3)$ eV.

DLTS spectra of 6*H*-SiC taken during the transmutation of W to Hf are shown in Fig. 4. There are several large peaks in the spectra that remain perfectly constant during the observation time. In Fig. 4(b), two regions of the spectrum are enlarged. Around 470 K, there is one peak labeled B_6 that

TABLE I. Parameters of tungsten-related band-gap states: thermal activation energy of electron emission and electron capture cross section σ (assumed to be independent of temperature). The errors given include all measured samples.

Polytype	Label	Energy (eV)	Capture cross section (10^{-12} cm^2)
4*H*	A_4	0.17(1)	0.01–0.06
	B_4	1.43(4)	0.3–2
6*H*	B_6	1.16(3)	0.4–1
15*R*	B_{15}	1.14(3)	0.4–1

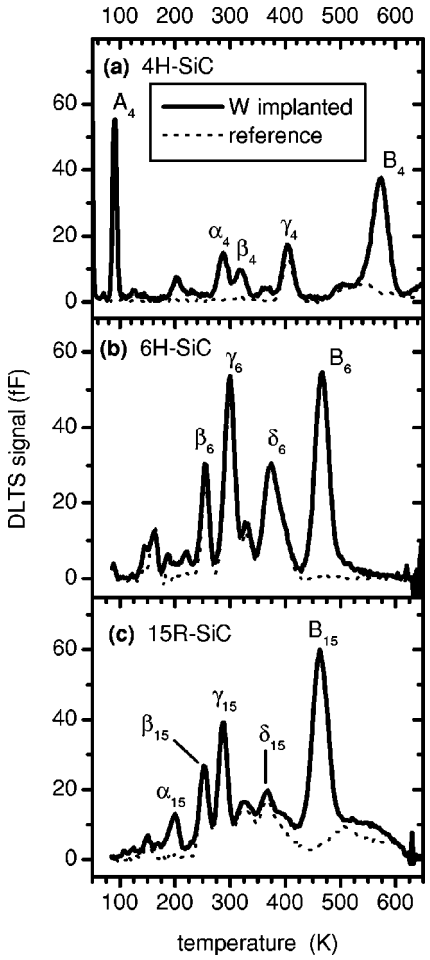

FIG. 5. DLTS spectra of *n*-type SiC (polytypes 4*H*, 6*H*, and 15*R*) implanted with stable tungsten isotopes. The dotted lines are reference spectra from an unimplanted area of each sample.

vanishes during the observation time. The corresponding trap parameters are $E = 1.16$ eV and $\sigma = (0.4–1) \times 10^{-12}$ cm^2. The height decreases exponentially with the expected half-life as demonstrated in Fig. 2(b), again proving the involvement of one W atom. Around 200 K, there are two tiny signals decreasing within the first delay time interval (16 d). As already discussed before, this effect is due to the unintentional ^{177}Ta contamination in the sample. This interpretation is supported by further doping experiments with stable Ta that reveal a slightly split Ta-related level ($E_C - 0.46$ eV and $E_C - 0.49$ eV, corresponding to the peak temperatures of 185 and 210 K in Fig. 4) in 6*H*-SiC.[28]

In addition to the time-dependent peaks identified as Ta or W related, there is a number of additional peaks in the spectra. Labeled with Greek letters and an index specifying the polytype, their level parameters are summarized in Table II. For several of them, the level parameters reasonably agree with defects that have already been observed in other experiments[29–32] as indicated in the table. Definite defect identifications, however, are not available and shall not be discussed here. In any case, there is no peak increasing during the elemental transmutation. This indicates the nonexistence of a band-gap state of the daughter element hafnium in the part of the band gap accessible by our DLTS experiments.

TABLE II. Band-gap states of unidentified defects or impurities detected by DLTS in the present experiments. These states are not related to tungsten. The last column lists defect labels used by other authors for band gap states with identical or similar trap parameters.

Polytype	Label	Energy (eV)	Capture cross section ($10^{-14}\,cm^2$)	Related defects [reference]
4*H*	α_4	0.58(3)	0.9–1	ID_9 [30], 0.62 eV [32]
	β_4	0.68(2)	3–4	Z_1/Z_2 [29], Z_1[30], EH_2[31], 0.68 eV [32]
	γ_4	0.84(2)	1–2	RD_1 [30]
	δ_4	0.9–1.1[a]	≈0.01	RD_3 [30]
6*H*	β_6	0.52(2)	1–2	ID_7 [30], 0.51 eV [32]
	γ_6	0.63(2)	1–3	Z_1/Z_2 [29,30]
	δ_6	0.67(3)	0.02–0.04	
15*R*	α_{15}	0.41(2)	2–4	
	β_{15}	0.50(3)	0.2–1	
	γ_{15}	0.62(1)	3–5	
	δ_{15}	0.65(2)	0.02–0.03	

[a]Level δ_4 consists of several (at least 2) components within the specified energy range.

IV. DLTS AND ADMITTANCE SPECTROSCOPY ON STABLE TUNGSTEN ISOTOPES

DLTS spectra from three polytypes doped with stable W are displayed in Fig. 5 together with reference spectra from unimplanted areas of the same samples. For each polytype, implantation-induced peaks show up in addition to peaks already present in the unimplanted material (for trap parameters, see Table II). The peaks A_4, B_4, and B_6, which are already identified to be W-related by the radiotracer experiment, clearly appear. Their level parameters agree within experimental errors with those obtained from the radiotracer experiments (Fig. 3). In the polytype 15*R*, the dominating implantation-induced peak B_{15} is at 470 K with a concentration and level parameters quite similar to the identified W peak B_6 in polytype 6*H*. Its parameters in polytype 15*R* are $E=1.14(3)$ eV and $\sigma=0.6\times10^{-13}\,cm^2$. By analogy to the polytypes 4*H* and 6*H*, we assign this level to a W-related defect. Further evidence for this assignment will become obvious from the discussion of the polytype dependence given below.

Some additional information on the four W-related levels (A_4, B_p with $p=\in\langle4,6,15\rangle$) can be obtained by varying DLTS measuring parameters as described in the following paragraphs. These measurements are performed on samples doped with stable W, because of the higher concentration and the known homogeneous depth profile of tungsten in these samples.

The capture process on all W-related levels was investigated by variation of the filling pulse length from 50 ns to 100 ms. For all polytypes and all W-related levels, no indications of a partial trap filling were found, i.e., the capture time constant is less than the minimum pulse length of 50 ns. From this experimental finding, a lower limit for the true capture cross for electrons section can be derived which is, at least, $2\times10^{-16}\,cm^2$. This lower limit is well compatible with the much larger (effective) capture cross sections derived from the usual DLTS Arrhenius evaluation of trap parameters (Table I).

The concentration of deep levels was derived from the DLTS spectra as shown in Fig. 5 and from DLTS depth profiling.[33] The concentration of the W-related levels is in the range of $(0.6–1)\times10^{14}\,cm^{-3}$, which is a factor 2–3 less than the nominally implanted W concentration. Taking into account systematic errors of at least a factor of 2 for absolute concentrations derived from DLTS measurements and additional errors (20%) in the determination of the very low implantation fluences, the difference is hardly significant.

The dependence of the emission time constant on the electric field strength within the Schottky diodes was investigated by variation of the reverse bias (up to 20 V) and pulse bias voltages. By taking differences between two transients taken with fixed reverse bias but slightly different pulse voltages, a narrow interval of the field strength is selected.

For the deep levels B_p common in all polytypes, the emission time constant remains perfectly constant (within 10%) if the field strength is varied. The range of field strengths accessible was [60; 160] kV/cm in the polytype 4*H*, [30; 100] kV/cm in 6*H*, and [20; 44] kV/cm in 15*R* (lowest field strength because of the low shallow doping level of the 15*R* samples). For the level A_4, however, a significant acceleration of the emission process with increasing field strength takes place as shown in Fig. 6. As an attempt, we tried to interpret this result as a Poole-Frenkel effect, i.e., a field-induced barrier lowering of a Coulomb center. However, the experimentally observed influence is significantly weaker than the theoretical expectation[34] (solid line in Fig. 6) for a singly charged center. If we nevertheless try to describe the experimental effect as a Poole-Frenkel effect, we may treat the effective charge q of the center as a free-fit parameter (dashed line in Fig. 6): this effective charge turns out to be only $0.2e$ (e is the elementary charge).

Though we do not know which mechanism[35] is actually responsible for the observed field dependence of level A_4, the weakness of the effect excludes an attractive Coulomb force between the center and the emitted electron, i.e. the center should be acceptorlike. For the deep W levels B_p, the interpretation as an acceptor state is even more convincing since these levels do not exhibit any field dependence at all.

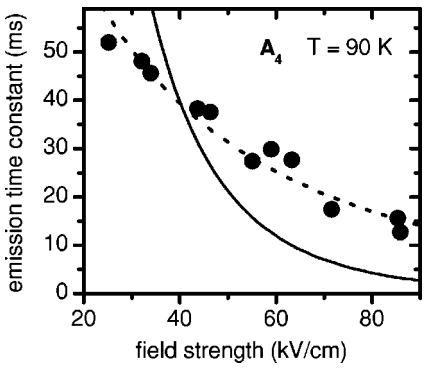

FIG. 6. Emission time constant of the level A_4 measured isothermally at 90 K with different electric field strength. The solid line displays the expected behavior for a singly charged donor center due to the field-induced barrier-lowering (Poole-Frenkel effect). The dashed line is a fit treating the effective charge q of the center as a free parameter (result $q=0.2e$).

This result is very similar to the behavior of Cr in 4H-SiC: both Cr and W have a level close to E_C with a detectable, but rather weak field-strength dependence, and a deeper level unaffected by an electrical field.[18] If both W levels in 4H-SiC are due to the same structural configuration (see discussion below), they are to be interpreted as a single (level B_4) and a double acceptor (level A_4) in close analogy to the case of chromium.[18]

The level A_4 was additionally investigated with TAS as shown in Fig. 7. To compensate for the lower sensitivity of TAS compared to DLTS, a higher tungsten concentration of $4\times10^{15}\,\mathrm{cm}^{-3}$ is used here. DLTS measurements on this type of sample are still possible (though not quantitative with respect to concentration) and reveal the same W levels A_4 and B_4 as described above. In Fig. 7, each step in the capacitance-versus-temperature curves and, equivalently, each peak in the conductance curves, corresponds to one band-gap state.[15] The leftmost two signals reflect the two levels of the nitrogen donors in the sample.[36] The third signal is not detectable in samples with low W concentration ($2\times10^{14}\,\mathrm{cm}^{-3}$) or in unimplanted samples and is therefore assigned to a W-related level.

Following the usual TAS data evaluation,[15] its energy is obtained from the slope of an Arrhenius plot of T^2/ω where T is the temperature of the characteristic step (or peak) and $\omega=2\pi f$ is the corresponding frequency. These data are included in the Arrhenius plot of Fig. 3(b) in order to compare them with the (T^2-corrected) emission time constant obtained by DLTS. The TAS data set has the same slope [activation energy 0.17(2) eV] as the DLTS data already discussed above, i.e., both DLTS and TAS reveal the same energy for the W level. The vertical offset between the TAS and the DLTS data sets in Fig. 3(b) corresponds to a factor of $\frac{1}{3}$. This difference is expected from TAS theory [Eq. (26) of Ref. 15], stating that

$$(T^2/\omega)_{\mathrm{TAS}}=\left(\frac{1}{2}\,\frac{1-\alpha}{1-s}\right)(T^2\tau)_{\mathrm{DLTS}}, \qquad (1)$$

where α is the concentration ratio of the deep W-related level under investigation (A_4) to the total (shallow plus deep) level concentration in the sample used for TAS. Here, we

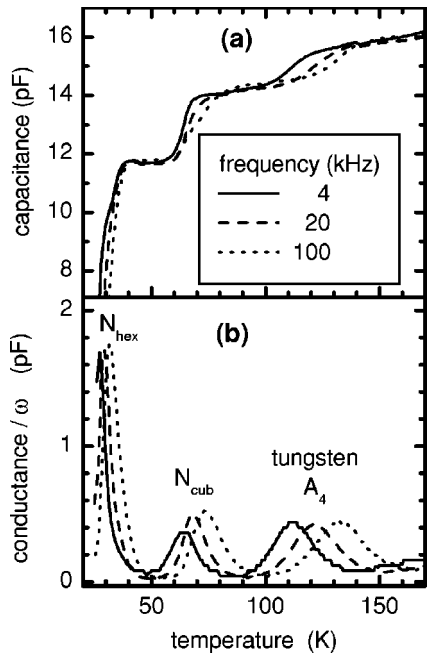

FIG. 7. Admittance spectroscopy on W-doped n-type 4H-SiC: (a) differential capacitance and (b) conductance as a function of temperature, measured with different frequencies.

estimate $\alpha=\frac{1}{3}$ since the implanted W concentration is one-half of the shallow doping concentration (nitrogen). The quantity s is the relative step height of the W-related step in the capacitance-versus-T curves and can be read from Fig. 7(a) to be $s=0.09$. Hence, the scaling factor in Eq. (1), relating the Arrhenius representation of TAS and DLTS data, is 0.37, in excellent agreement with the offset between the experimental data sets in Fig. 3(b).

V. DISCUSSION AND POLYTYPE DEPENDENCE

The radiotracer experiments provide a definite chemical identification of the discovered band-gap states A_4 and B_p with tungsten, i.e., these states are either due to one tungsten atom or, possibly, due to complexes containing exactly one W atom. The characteristic level parameters energy and capture cross section σ agree with the results obtained with stable W doping. They are summarized in Table I with error margins representing all measured samples. Due the missing or only weak influence of the electric field strength, all levels are interpreted to be acceptorlike.

In 4H-SiC, the question arises whether the two different band-gap states A_4 and B_4 belong to the same lattice site or structural configuration of a W atom or not. Within experimental errors (up to 50%), their concentrations are identical in each sample. This is a hint to the existence of one configuration only, with two energy levels in the accessible energy range. This is, however, not definite proof, since the comparison of concentrations (implanted W atoms versus W-related gap states) is quite inaccurate and always exhibits a deficit of gap states, i.e., the existence of more than one W configuration cannot be excluded.

In particular, there is no definite criterion to decide whether the observed tungsten-related levels are due to isolated impurities or due to complexes involving one W atom.

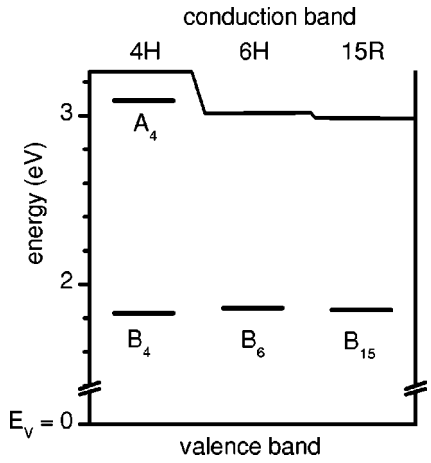

FIG. 8. Energy scheme of tungsten-related levels in the SiC polytypes 4*H*, 6*H*, and 15*R*. The lower part of the band gap has not been investigated.

A hint, at least, favoring isolated tungsten impurities is given by the following argument: the W-related levels themselves, their degree of electrical activation, and, in the polytype 4*H*, their concentration ratios are well reproducible though the implantation fluence of tungsten varies by two orders of magnitude and though the damage produced by the radiotracer implantation is heavier (due to additional coimplanted ions) compared to the implantation of stable isotopes. If the observed W-related levels were due to complexes with implantation defects, we would not expect this reproducibility. However, complexes with other defects (intrinsic or extrinsic) cannot be excluded.

Now, we are going to discuss the polytype dependence of the level position (Fig. 8). According to Langer and Heinrich,[37] deep levels may serve as a common reference level to adjust the energy scales in different crystals towards each other. Applying this rule to deep states of V and Cr in SiC, we recently predicted[19] the conduction band offset between 4*H*- and 6*H*-SiC to be 0.22(6) eV. Alternatively, we are now going to assume that the valence-band edges are aligned in different polytypes as predicted from experiments by Avanas'ev *et al.*[38] Then, the conduction-band offset between the polytypes is identical to the difference in the gap width. Using $E_{\mathrm{gap}}=3.26$, 3.02, and 2.99 eV for the polytypes 4*H*, 6*H*, and 15*R*,[39] the conduction-band offsets are 0.24 eV (4*H*-6*H*) and 0.03 eV (6*H*-15*R*). These numbers correspond well to the difference in energy of the deep W levels B_p (Table I, measured relative to the conduction band), i.e. the levels appear well aligned in different polytypes if drawn with respect to a common valence band edge (Fig. 8). This result means that the Langer-Heinrich rule and the assumption of zero valence-band offset are well compatible. It also explains why an additional band-gap state A_4 of W is observed in the polytype 4*H* only: in 6*H*- and 15*R*-SiC, the corresponding state does not fit into the band gap.

Next, we are going to discuss a possible level splitting due to the inequivalent lattice sites on each sublattice (C or Si). There are two different sites in the 4*H*, three sites in the 6*H*, and five sites in the 15*R* polytype. The occupation of these different sites may result in the formation of energetically different band-gap states. This is well known and theoretically understood for shallow donors (N and P).[40] The effect is also obvious in Fig. 7 where two different nitrogen levels appear due to the occupation of quasihexagonal and quasicubic sites. A level splitting due to inequivalent sites has also been reported for several deep levels, e.g., of the impurities titanium,[18,41] vanadium,[19,42] and chromium.[18] In the present case of tungsten, no splitting is resolved by DLTS; instead, the tungsten peaks appear slightly broadened compared to the ideal peak shape. To give a quantitative measure, we arbitrarily tried to simulate the peak width by a superposition of two adjacent levels with identical concentration and capture cross section. With these assumptions, the result is a level splitting of 0.03(1) eV for the deep B_p levels. For the A_4 level, the upper limit for an eventually unobserved splitting is 0.01 eV. At present, we do not have a detailed understanding of level splitting of deep levels and its polytype dependence. Empirically, we compare tungsten to the isovalent chromium and to its neighboring element Ta, but no general rule will become obvious. The level scheme[18,19] of Cr in the upper part of the band gap also consists of a deep acceptor (in 4*H*, $E_C-0.74$ eV, no splitting detectable) and a second state (interpreted to be the corresponding double-acceptor state) quite close to the conduction band of the 4*H* polytype, which is—in contrast to the A_4 level of tungsten—clearly split by 0.04 eV. The donor state of Ta is clearly split in the 6*H* polytype by 0.03 eV [see Sec. III and Fig. 4(b)]. Hence, the absence or smallness of the level splitting of tungsten should not be ascribed to the large atomic size of such heavy elements and an eventually resulting lattice relaxation that might dominate over the crystallographic inequivalence of different sites. Such arguments would apply to Ta as well.

Finally, we are going to predict macroscopic electrical properties of W-doped SiC. The deep W level B_p, if empty, will act as a very efficient capture center for electrons due to its huge capture cross section, i.e., minor traces of W will drastically reduce the electron (minority-carrier) lifetime in *p*-type SiC. In *n*-type SiC, the deep W level will act as a compensating acceptor. If the concentration of the deep B_p level exceeds the concentration of shallow donors, all electrons should be trapped in this state. Hence, the material should become semi-insulating with a very high activation energy of 1.4 eV (polytype 4*H*), which guarantees that this insulating property withstands high temperatures as it is desired for applications. This expectation renders W an excellent candidate for the production of semi-insulating SiC. The practical feasibility of this idea, however, depends on the still unknown solubility of W in SiC and the availability of a practicable doping process.

This scenario for W is quite different from the expected behavior of the adjacent element tantalum, which, according to the electrical field influence observed by DLTS, is expected to act as a donor (0.68 eV below E_C).[11] In this case, no significant effect of tantalum contamination on electrical conductivity is expected in *n*-type material, i.e., some Ta contamination due to Ta-containing growth equipment is expected to be acceptable.

Hafnium does not have a band-gap state in the part of the SiC band gap accessible by our experiments. Carefully speaking, this result applies to Hf in 4*H*- and 6*H*-SiC, which is formed by the nuclear transmutation of electrically active Ta or W to Hf. In principle, this configuration (e.g.,

lattice site, complex formation) of Hf may be different from the one that might exist after doping during growth or unintentional incorporation.

VI. CONCLUSIONS

Band-gap states of tungsten in the upper part of the band gap have been characterized in the polytypes $4H$, $6H$, and $15R$ of silicon carbide. Due to the radiotracer concept used, the chemical identification is definite, i.e., there is exactly one W atom involved. The involvement of another impurity or defect in the electrically active center is unlikely, but cannot be excluded definitely. In all polytypes investigated, tungsten has a deep acceptor level with a large capture cross section of $10^{-12}\,\mathrm{cm}^2$. Relative to the conduction-band edge E_C, the level energies are $-1.43(4)$, $-1.16(3)$, and $-1.14(3)$ eV in the polytypes $4H$, $6H$, and $15R$, respectively. In the polytype with the largest band gap, $4H$, an additional level at $E_C-0.17(1)$ eV exists. Due to the deep acceptor level, tungsten is a promising candidate for the production of semi-insulating SiC via an intentional compensation of *n*-type SiC.

ACKNOWLEDGMENTS

We thank H. Hobert for the polytype determination by Raman spectroscopy and D. Siche (Institute of Crystal Growth, Berlin) for stimulating discussions on the relevance of Ta and W for SiC crystal growth. U. Reislöhner developed software for TAS measurement and evaluation. The work was funded by the German BMBF and by the Deutsche Forschungsgemeinschaft (DFG, SFB 196).

*Present address: Fraunhofer Institute for Integrated Circuits IIS-A, Am Weichselgarten 3, D-91058 Erlangen, Germany.
†Corresponding author, Email: pasold@pinet.uni-jena.de

[1] H. Morkoc, S. Strite, G. B. Gao, M. E. Lin, B. Sverdlov, and M. Burns, J. Appl. Phys. **76**, 1363 (1994).
[2] R. R. Siergiej, R. C. Clarke, S. Sriram, A. K. Agarwal, R. J. Bojko, A. W. Morse, V. Balakrishna, M. F. MacMillan, A. A. Burk, Jr., and C. D. Brandt, Mater. Sci. Eng., B **61–62**, 9 (1999).
[3] *Properties of Silicon Carbide*, edited by G. L. Harris, Emis Datareviews Series No. 13 (INSPEC, London, 1995).
[4] J. A. Cooper, Jr., M. R. Melloch, J. M. Woodall, J. Spitz, K. J. Schoen, and J. P. Henning, Mater. Sci. Forum **264–268**, 895 (1998).
[5] C. E. Weitzel, Mater. Sci. Forum **264–268**, 907 (1998).
[6] D. M. Brown, E. Downey, M. Ghezzo, J. Kretchmer, V. Krishnamurthy, W. Hennesy, and G. Michon, Solid-State Electron. **39**, 1531 (1996).
[7] R. Schorner, P. Friedrichs, D. Peters, and D. Stephani, IEEE Electron Device Lett. **20**, 241 (1999).
[8] Yu. A. Vodakov, A. D. Roenkov, M. G. Ramm, E. N. Mokhov, and Yu. N. Makarov, Phys. Status Solidi B **202**, 177 (1997).
[9] M. S. Ramm, E. N. Mokhov, S. E. Demina, M. G. Ramm, A. D. Roenkov, Yu. A. Vodakov, A. S. Segal, A. N. Vorob'ev, S. Yu. Karpov, A. V. Kulik, and Yu. N. Makarov, Mater. Sci. Eng., B **61–62**, 107 (1999).
[10] L. B. Rowland, G. T. Dunne, and J. A. Freitas, Jr., Mater. Sci. Forum **338–342**, 161 (2000).
[11] J. Grillenberger, N. Achtziger, R. Sielemann, and W. Witthuhn, J. Appl. Phys. **88**, 3260 (2000).
[12] O. Noblanc, C. Arnodo, C. Dua, E. Chartier, and C. Brylinski, Mater. Sci. Eng., B **61–62**, 339 (1999).
[13] D. V. Lang, J. Appl. Phys. **45**, 3023 (1974).
[14] P. Blood and J. W. Orton, *The Electrical Characterization of Semiconductors: Majority Carriers and Electron States* (Academic, London, 1992), p. 344 and p. 426.
[15] J. L. Pautrat, B. Katircioglu, N. Magnea, D. Bensahel, J. C. Pfister, and L. Revoil, Solid-State Electron. **23**, 11 59 (1980).
[16] P. Blood and J. W. Orton, Ref. 14, p. 492.
[17] J. W. Petersen and J. Nielsen, Appl. Phys. Lett. **56**, 1122 (1990).
[18] N. Achtziger and W. Witthuhn, Phys. Rev. B **57**, 12 181 (1998).
[19] N. Achtziger, J. Grillenberger, and W. Witthuhn, Mater. Sci. Forum **264–268**, 541 (1998).
[20] N. Achtziger, Mater. Sci. Forum **248–249**, 113 (1997).
[21] N. Achtziger, J. Grillenberger, and W. Witthuhn, Hyperfine Interact. **120/121**, 69 (1999).
[22] N. Achtziger, H. Gottschalk, T. Licht, J. Meier, and M. Rüb, U. Reislöhner, and W. Witthuhn, Appl. Phys. Lett. **66**, 2370 (1995).
[23] R. B. Firestone and V. S. Shirley, *Table of Isotopes* (Wiley, New York, 1996).
[24] U. Reuss and W. Westmeier, At. Data Nucl. Data Tables **29**, No. 1 (1983).
[25] J. Bourgoin and M. Lanoo, *Point Defects in Semiconductors II* (Springer, Berlin, 1983), p. 177.
[26] G. L. Miller, D. V. Lang, and L. C. Kimmerling, Annu. Rev. Mater. Sci. **7**, 377 (1977).
[27] Model DL8020 from Biorad Ltd. (Great Britain) or PhysTech (Germany). The capacitance is measured by a Boonton capacitance bridge with a 100 mV, 1 MHz test signal and digitized for further data processing.
[28] J. Grillenberger, Ph.D. thesis, University of Jena, Germany (2000).
[29] A. A. Lebedev, Semiconductors **33(2)**, 107 (1999).
[30] T. Dalibor, Phys. Status Solidi A **162**, 199 (1997).
[31] C. Hemmingson, N. T. Son, O. Kordina, E. Janzén, J. L. Lindström, S. Savage, and N. Nordell, Mater. Sci. Eng., B **46**, 336 (1997).
[32] J. P. Doyle, M. O. Aboelfotoh, and B. G. Svensson, Mater. Sci. Forum **264–268**, 565 (1998).
[33] D. Stievenard and D. Vuillaume, J. Appl. Phys. **60**, 973 (1986).
[34] J. L. Hartke, J. Appl. Phys. **39**, 4871 (1968).
[35] P. A. Martin, B. G. Streetman, and K. Hess, J. Appl. Phys. **52**, 7409 (1981).
[36] A. O. Evwaraye, S. R. Smith, W. C. Mitchel, and M. D. Roth, Appl. Phys. Lett. **68**, 3159 (1996).
[37] J. M. Langer and H. Heinrich, Phys. Rev. Lett. **55**, 1414 (1997).
[38] V. V. Afanas'ev, M. Bassler, G. Pensl, M. J. Schulz, and E. Stein von Kamienski, J. Appl. Phys. **79**, 3108 (1996).
[39] S. Yoshida, in Ref. 3, p. 74.
[40] W. Kohn and J. M. Luttinger, Phys. Rev. **98**, 915 (1955).
[41] T. Dalibor, G. Pensl, N. Nordell, and A. Schöner, Phys. Rev. B **55**, 13 618 (1997).
[42] V. A. Il'in and V. A. Ballandovich, Defect Diffus. Forum **103–105**, 633 (1992).